Bull. Astr. Soc. India (2003) **31**, 49–64

NGC 1245 - an intermediate age open cluster

Annapurni Subramaniam[1]*

[1] *Indian Institute of Astrophysics, II Block Koramangala, Bangalore 560 034, India*

Received 2 December 2002; accepted 12 March 2003

Abstract. The B,V CCD photometry of 916 stars in the field of the high galactic latitude intermediate age open cluster NGC 1245 is presented. The cluster parameters were estimated with the help of V vs (B−V) colour magnitude diagram (CMD). After correcting for intra-cluster reddening, the mean redding towards the cluster was found to be 0.29±0.05 mag, with a distance modulus $(m-M)_0$ equal to 12.4±0.3 mag. The cluster is found to be located at a distance of 3 Kpc. The isochrone fits using Girardi et al. (2000) isochrones to the cluster CMD estimated an age of 890±100 Myr. The synthetic CMDs obtained using Girardi et al. (2000) models incorporating photometric errors and 10% binary stars estimated an age of 1 Gyr for the cluster. The luminosity function (LF) of the main-sequence shows dips, which might arise due to some known gaps in the main-sequence, including the Bohm-Vitense gap. The LF and integrated LF computed from the observed CMD is compared with those computed from the synthetic CMDs for five values of the mass function. The estimation of the present day mass function indicates a flatter value compared to the Salpeter value, though an accurate estimation is not possible due to the large dips found in the LF. The apparent paucity of brighter stars seen near the cluster center is estimated to have a statistical significance of 2 σ.

Keywords : Open cluster – NGC 1245 – interstellar reddening – distance – age – mass function

1. Introduction

The open star cluster system of our Galaxy is one of the important constituent of the disk of the Galaxy. The open star clusters are formed from molecular clouds at the sites of star formation.

*e-mail: purni@iiap.ernet.in

In general, the open star clusters are found very close to the plane of the galaxy, typical scale height being, 100 – 200 pc. Some open clusters are found to be located away from the disk of the Galaxy, more than the scale height. NGC 1245 is an intermediate age star cluster situated close to the Perseus spiral arm and is located 444 pc below the plane of the Galaxy. The location of this cluster and its irregular appearance got us interested in this cluster. NGC 1245 (RA = 3h 11.2m; Dec = +47 4) is located away from the center of the Galaxy (l=146.6; b=-8.9). This intermediate age cluster might belong to the old disk population with a larger scale height of about 500 pc. The intermediate age clusters located far away from the galactic plane could also throw some light about the old disk or the thick disk population of the Galactic disk.

This cluster has been studied previously by Hoag et al. (1961) and Chincarini (1964). The cluster finding chart presented by Hoag et al. (1961) shows that the cluster seems to lack stars near the cluster center. Another study of this cluster based on CCD BV photometry is done by Carraro & Patat (1994). They obtain a colour excess E(B−V) = 0.26 mag and an apparent distance modulus (m−M) = 13.20 mag. Wee & Lee (1996) have carried out Washington CCD photometry of this cluster and found that this cluster is not metal rich, given in the Lyngå (1987) catalogue. A comparison with the photographic data given at the site WEBDA, indicates that there may be calibration problems in Carraro & Patat data. This has also been indicated by Wee & Lee (1996). Therefore, we present a new set of CCD photometry for the stars in the region of NGC 1245. The cluster colour-magnitude diagrams (CMDs) are used to estimate the reddening, age and distance to the cluster. The synthetic CMDs are used to estimate luminosity functions in order to compare with the observed ones and also to estimate the present day mass function of the cluster.

2. Observation and data analysis

The cluster was observed from the 2.34m Vainu Bappu Telescope at Kavalur, India during the 1-4 Jan 2000 observing run. The observational log is presented in Table 1. We used a 1K x 1K CCD camera at the prime focus, with an image scale of 0."63 arcsec/pix. The night of observation was not photometric and hence we used the stars observed by Hoag et al. (1961) as calibration stars. The CCD data were calibrated using IRAF data reduction package. The instrumental magnitudes were estimated using the DAOPHOT II package. The zero point errors are of the order of 0.02 mag. The V magnitude and (B−V) colour are estimated for 916 stars. The present data is compared with the CCD data of Carraro & Patat (1994) and the results are shown in Figure 1. The differences are computed as present data minus Carraro & Patat (1994) data, and the difference is plotted against the respective magnitude or colour. The average value of δV is found to be 0.01 mag, with $\sigma = 0.04$ mag, and the average value of $\delta(B-V)$ is 0.04 mag, with $\sigma = 0.02$ mag. The colour plot shown in the bottom panel of Figure 1 shows that the colour difference has a colour dependence, indicating colour calibration problems with Carraro & Patat (1994) data.

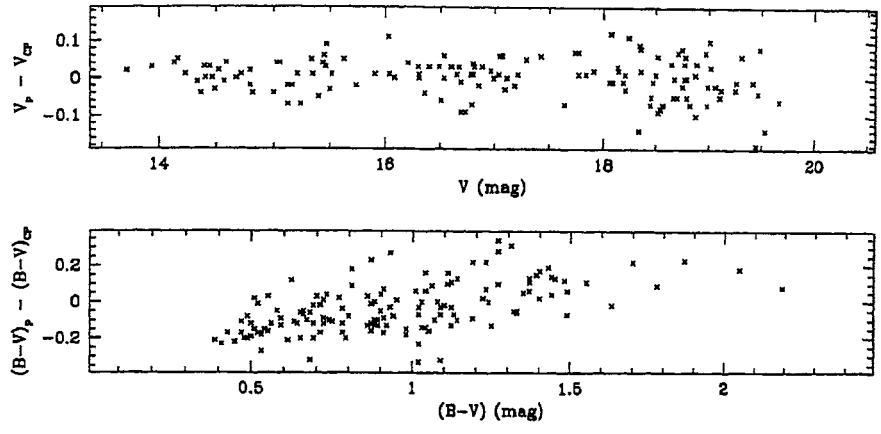

Figure 1. The present data is compared with the data from Carraro & Patat (1994) and the results are presented here. Carraro & Patat (1994) data is subtracted from the present data and the difference is shown as a function of the present colour/magnitude.

Table 1. Journal of observation.

Date	Filter	UT	Airmass	Exp. Time (Sec)
Jan 02 2000	B	14 21	1.51	60.0
Jan 02 2000	B	14 23	1.50	300.0
Jan 02 2000	B	14 32	1.48	1200.0
Jan 02 2000	V	13 45	1.58	60.0
Jan 02 2000	V	13 48	1.57	300.0
Jan 02 2000	V	13 58	1.53	900.0

3. Data incompleteness

In general, the incompleteness in the photometric data is a function of stellar crowding and stellar magnitudes. In the case of open clusters, the crowding is very minimal and hence the incompleteness is mainly a function of the stellar magnitudes. We estimated the completeness of the photometric data in both B and V passbands in the long exposure frames. The completeness in the data changes slightly from the center of the frame to the periphery. Hence the data completeness for the cluster and the field region are tabulated in table 2.

The observed region of the cluster is shown in Figure 2. The cluster center as found by Carraro & Patat (1994) is denoted by a big open circle. We used this as the cluster center and

Table 2. The data completeness in B and V pass bands in percentage for the cluster and field regions are tabulated here.

B(mag)	cluster CF	field CF	V (mag)	cluster CF	filed CF
upto 18.0	100.0	100.0	upto 17.0	100.0	100.0
18.0 – 19.0	99.0	100.0	17.0 – 18.0	98.0	98.0
19.0 – 20.0	98.4	99.2	18.0 – 19.0	96.0	97.0
20.0 – 21.0	94.0	94.0	19 – 19.5	95.0	96.5

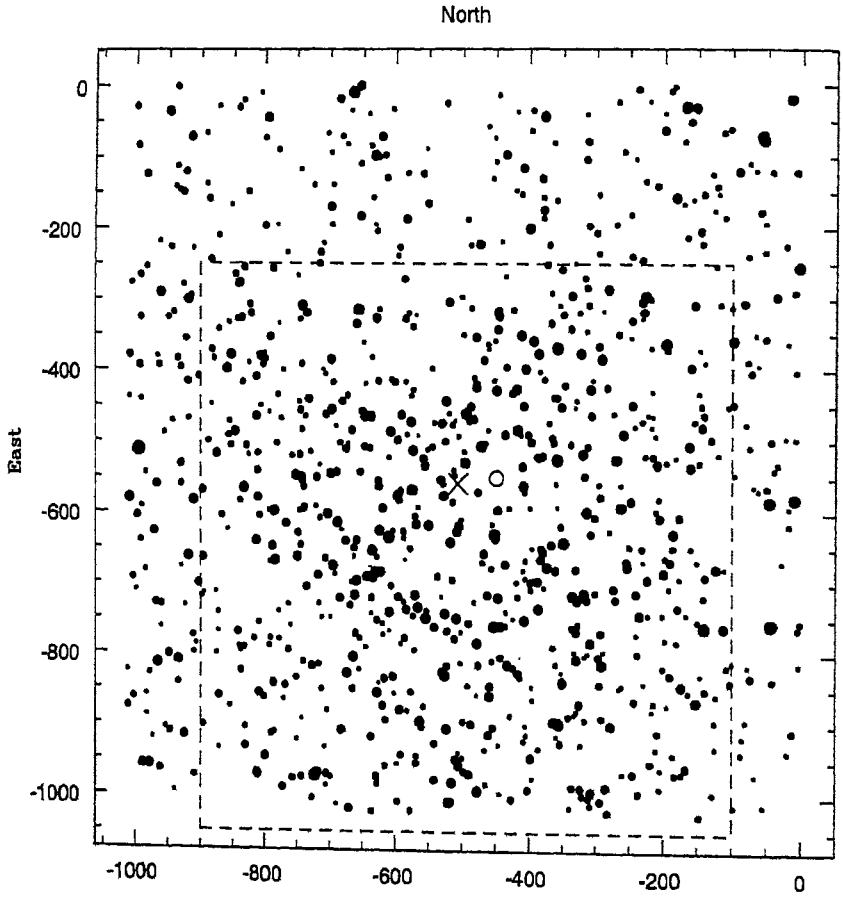

Figure 2. The observed region of the cluster NGC 1245 is shown in the Figure. The cluster is assumed to be confined within the dashed lines. The cluster center as found by Carraro & Patat (1994) is denoted by a big open circle. The center found in the present analysis is denoted by cross.

re-estimated the cluster center using all the observed stars. The center thus found is marked by a cross. It can be clearly seen from the cluster plot that the brighter cluster members are confined within a radius of around 400 pixels. Thus we have assumed that the cluster occupies the area within the dashed lines and the region outside the dashed box represents the field region. We estimate the field star contamination in the cluster region using the data in this region.

4. Structure of the cluster

From the cluster plot as shown in Figure 2, it can be seen that the cluster seems to lack stars near the center and also, the stars seem to be distributed in an annulus. The cluster center as found by Carraro & Patat (1994) is denoted by a big open circle. We used this as the cluster center and re-estimated the cluster center using all the observed stars. The center thus found is marked by a cross. We estimate the radial density profile (RDP) to study the radial density structure of the cluster. The stellar density are estimated in radial bins from the center. We computed the RDP for radial bins of 0.5 and 1 arcmin. RDP were estimated including all stars and also for stars brighter than 17 mag. Two reasons for considering only brighter stars: (a) to estimate the statistical significance of the apparent paucity of bright stars near the cluster center and (b) brighter star RDP could be used to identify the presence of mass segregation in the cluster. When estimating the RDP for all stars, the incompleteness in the data is incorporated. The radial density profiles are shown in Figure 3, the density in the left panels is estimated using a radial bin of 1 arcmin and that in the right panels using 0.5 arcmin. The top panels show the RDP computed using all the stars and the lower panels show the RDP computed using stars brighter than 17.0 mag.

It can be seen that the RDP in the top left panel is very smooth. This profile is very similar to the RDP presented by Nilakshi et al. (2002), in their Figure 1. The top right panel shows a smooth profile outside 2 arcmin radius, but the profile shows fluctuation near the center. This dip in the RDP is not seen by Nilakshi et al. (2002) as they consider all stars with 1 arcmin radial bin and the dip is mainly seen in the RDP of stars brighter than 17 mag. The RDP are fitted with the function $\rho(R) \propto f_0/(1+(R/R_0)^2)$, where R_0 is the core radius, at which the density $\rho(R)$, becomes half of the central density, f_0. These are also plotted in Figure 3, shown as dotted lines. In the case of top-left panel, the fit is extremely good with a χ^2 value of 0.15. The core radius is found to be 4.75 arcmin. In the case of the lower-left panel, the fit to all the points turned out to be quite unsatisfactory, with a χ^2 value of 2.1. Instead, we fitted the function to the points except the one at 1 arcmin, then the χ^2 value was found to be 0.4. This fit gives a core radius of 3.1 arcmin, which is much lower than the value obtained when all stars were considered. If the fitted function were to extend to the inner radii, at 1 arcmin, the observed density is found to be lower than the computed density. The difference is about 1.6 σ. Hence RDP with 1arcmin radial bins for stars brighter than 17 mag suggest that the central 2 arcmin has less number of brighter stars than what is expected. The RDP computed with half arcmin radial bins also show the fluctuation in the number density of stars near the center. This is much more pronounced in the lower-left panel, where stars brighter than 17 mag are considered. The RDP model profile, computed for the lower-left panel is over plotted on the lower-right panel. The observed number

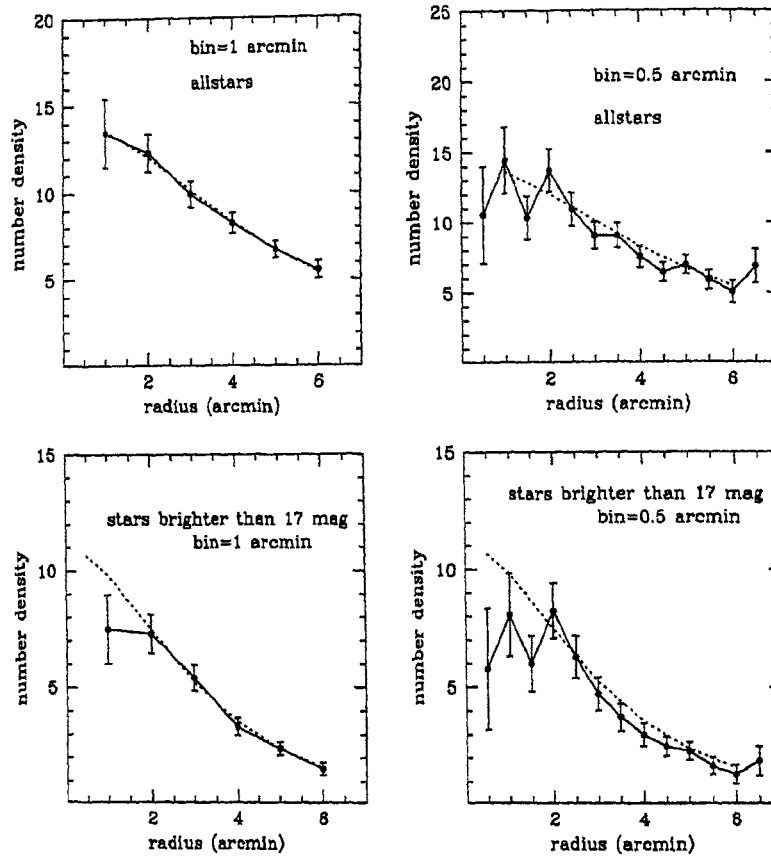

Figure 3. The radial density of the cluster as a function of the radius is shown in bold line. The left panel is for a radial bin of 1 arcmin and the right panel for a radial bin of 0.5 arcmin. The dotted line shows the fitted profile.

density at 0.5 arcmin radius is seen to be lower than the value expected by the fit, lower by 2 σ. Hence this strengthens the point that the central density of bright stars is likely to be less than what is expected.

The dip in the RDP could also be due to choice of center of the cluster. The estimated cluster center is shown in Figure 2. This center was shifted by 50 pixels (0.5 arcmin) in all the four directions and the RDP was re-estimated for stars brighter than 17 mag and with 0.5 arcmin bin. The central dip in the profile was observed in three of the four RDP with shifted centers. Three

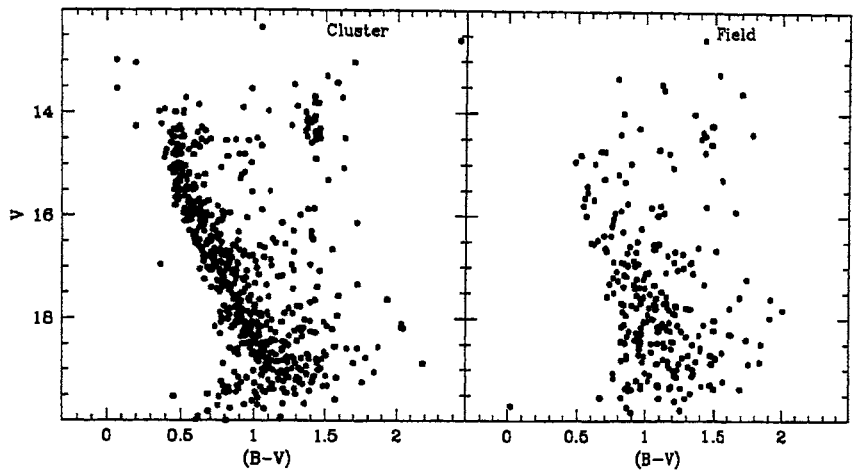

Figure 4. The Colour Magnitude diagram of the cluster region and the field region are shown here.

RDPs with shifted centers showed a central density dips which are more then 1 σ, indicating that the choice of the center is not the reason for the observed dip in the central density of stars brighter than 17 mag.

As this cluster is known to be an intermediate age cluster, the n-body relaxation within the cluster would have resulted in the segregation of brighter stars towards the center of the cluster. This would result in a steeper RDP for brighter stars. This may be the reason for obtaining a lower value of core radius for brighter stars. On the other hand, the bright star RDP is seen to be shallower than the fitted function in the central regions, though the statistical significance is not very high (2 σ). Also this result is independent of the errors in choosing the cluster center. Hence the apparent paucity of brighter stars near near the cluster center has 2 σ significance.

5. Colour-Magnitude Diagram

The parameters of the cluster can be estimated using the CMD. The V vs (B−V) CMD is shown in Figure 4. The left side shows the CMD for the cluster region with 659 stars and the right side for the field region with 257 stars. The cluster CMD spans between V=13 – 19.5 mag and a few red giants are seen at V= 14 mag and (B−V) = 1.4 mag. A broad main-sequence (MS) is seen, with a large number of stars near the turn-off. One of the reasons for the scatter on the MS is the presence of differential reddening across the face of the cluster, apart from the presence of binaries. The differential reddening on the face of this cluster was noticed earlier by Carraro & Patat (1994). An estimate of this is required to obtain a more tight MS and thus to obtain more accurate estimation of the cluster parameters.

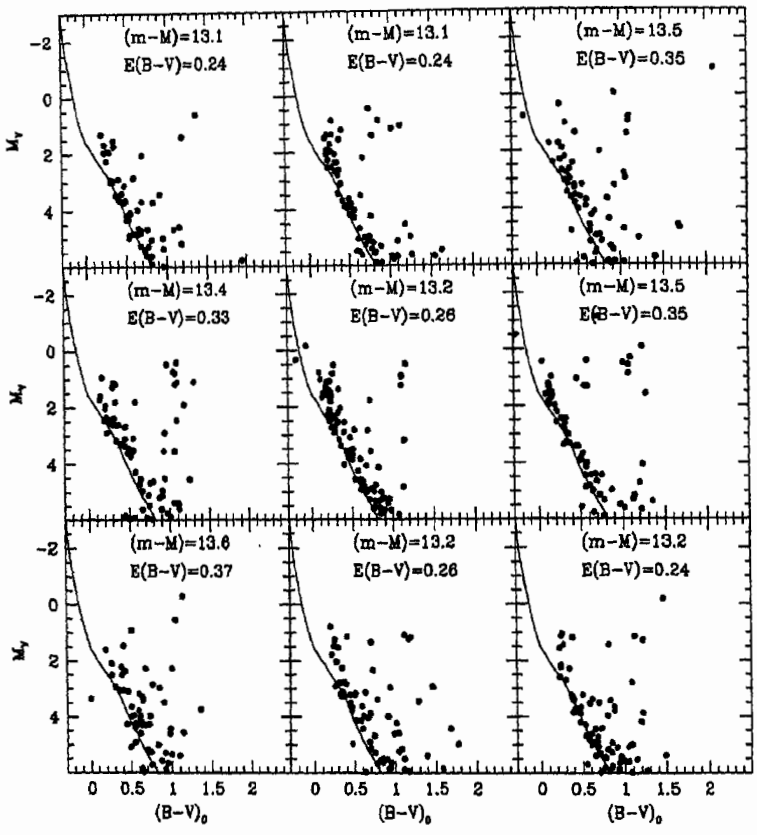

Figure 5. The ZAMS fit to the 9 cluster regions are shown here. The estimated reddening and distance modulus for each region are indicated.

5.1 Differential reddening

In order to estimate the amount of differential reddening, we divide the cluster region into 9 equal regions. The CMDs for stars within each region are constructed and fitted with ZAMS to estimate the individual redding and distance modulus. The corresponding CMDs are shown in Figure 5, fitted with ZAMS. The estimated values of reddening E(B−V) and the apparent distance moduli are also shown.

It can be seen that there is a significant amount of differential reddening across the face of

the cluster with the minimum and the maximum values of reddening being 0.24 and 0.37 mag respectively. It must be noted that the values estimated for each region may also be an average in itself. Further refinement in the estimate is not possible as the number of stars per region becomes too small to reliably estimate reddening. Using the estimated individual reddening per region, the stars in each region are de-reddened and are also corrected for extinction. The cluster CMD after the above procedure is seen to have reduced scatter in the MS. This CMD is used for further analysis. The mean reddening towards the cluster is estimated to be E(B−V)=0.29 ± 0.05 mag and the absolute distance modulus is 12.4±0.3 mag. This corresponds to a distance of 3020 pc, or 3 Kpc. The error involved in the estimation of distance modulus is 420 pc. The estimates of reddening and distance obtained here are in excellent agreement with the values obtained by Carraro & Patat (1994).

6. Cleaning the CMD

The CMD after the removal of the intra-cluster reddening has the following two defects. They are the presence of field stars and incompleteness in the stellar data. In order to overcome these problems, we used a statistical method. The method works as follows.

First, the CMDs of the field and the cluster regions are divided into various small boxes. These boxes have a width 0.25 mag in V and 0.2 mag in (B−V). The number of stars in each box is estimated. For each box, the data incompleteness values for the mean values of V and B magnitudes are estimated and the lower of the two values is adopted as the data incompleteness value for the box. Then the number of stars required to be added in each box in order to make the data complete, is calculated. These stars are then distributed randomly within the box. This procedure of adding extra stars in accordance with the incompleteness in the data in various regions of the CMD is done for both the cluster and the field CMDs. The area considered for field stars is less than cluster area and the cluster area is found to be 1.4 times more than the field area. Hence the number of stars in the field region needs to be multiplied by the above number to be able to compare the field CMD directly with the cluster CMD. Hence the extra stars arising out of the above factor is also randomly distributed within the boxes.

The next procedure is to remove the field stars from the cluster CMD, using a technique called zapping technique. A very similar procedure is used in the analysis of LMC clusters in Subramaniam & Sagar (1995). The cluster CMD contains cluster stars as well as field stars and these field stars are required to be removed to obtain a CMD with only cluster stars. In this method, for each star in the field CMD, the nearest star on the cluster CMD is removed. For a star in the field CMD, the same position on the cluster CMD is chosen and then the cluster CMD is searched for a star closest to this position by searching within a V vs (B−V) box and increasing the size of the box until a star is found. The range chosen to search for the star in the cluster CMD is a maximum of 1 mag in V and 0.5 mag in (B−V). This procedure is repeated for all the stars in the field CMD. Once all the thus identified field stars are removed from the cluster CMD corresponding to the stars in the field CMD, the resulting CMD can be considered to be devoid of field stars. This CMD is presented in Figure 6.

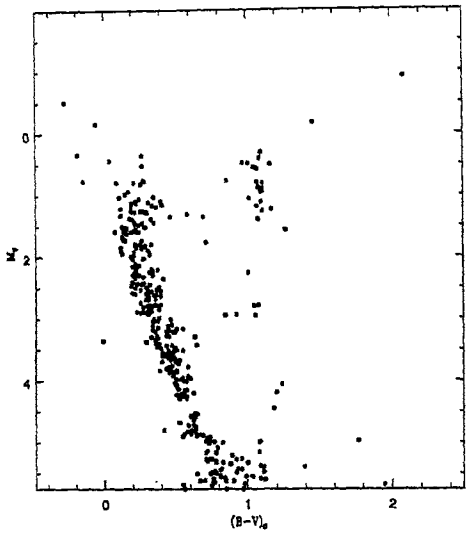

Figure 6. The CMD corrected for differential reddening, data incompleteness and field star contamination is shown here.

As the procedure adopted here is a statistical one, the stars which have the maximum probability to be a field star in the cluster CMD are removed. Therefore the probability of the presence of field stars in the final CMD is very less, though a few field stars still may be present. A look at the CMD presented in Figure 6 shows that the scatter seen at the top of the CMD remains the same, indicating that this truly is a cluster feature. The MS is quite narrow and much refined when compared to the cluster CMD, shown in Figure 4. The noticeable feature on the MS is the clumpy distribution of stars along the V magnitude and the sharp decrease in the number of stars near the limiting magnitude of the present analysis, that is $M_V = 5.7$ mag. The presence of a few stars near $M_V \sim 3.0$, 4.5 mag and $(B-V)_0 \sim 1.0$ mag can be noticed and these stars are most likely to be the left over field stars. On the whole this CMD can be assumed to consist only of cluster stars and hence this CMD is used for further analysis.

7. Estimation of Age

The CMD which is corrected for intra-cluster reddening, data incompleteness and field star contamination is used to estimate the age of the cluster. We used the isochrones from Girardi et al. (2000) for age estimation. Girardi et al. (2000) presented isochrones for Z= solar and Z=0.30 and also for sub-solar values of Z. The metallicity of the red giants in this cluster as estimated by Wee & Lee (1996) was [Fe/H] = -0.04±0.05 dex. This is very close to the solar value and hence we fit the solar metallicity isochrones. Girardi et al. (2000) isochrones for sub-solar value of Z is for

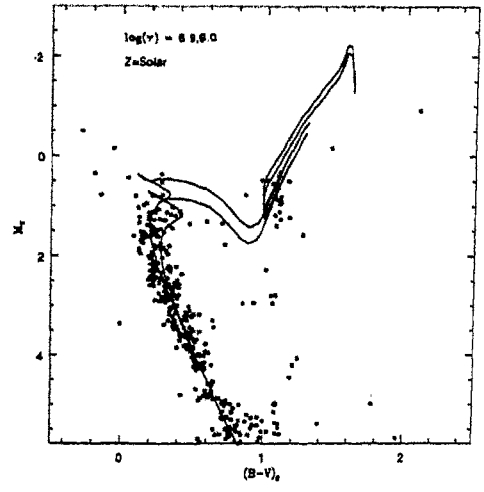

Figure 7. The age of the cluster is estimated by fitting the isochrones from Girardi et al. (2000).

0.008 which is equivalent to [Fe/H] of -0.4 dex and this is very much less than that estimated for the cluster. Hence we use only the solar metallicity isochrones. The isochrone fits for ages $log(\tau)$ = 8.9, 9.0 are shown in Figure 7. Two stars are seen brighter and redder than most of the red giants. From the isochrone fit, it is difficult to consider them as cluster members. A few stars are seen brighter than the MS turn-off, some of these might be candidate blue-stragglers. Hence we estimate an age of 890 ± 100 Myr for the cluster. The age estimated by Carraro & Patat (1994) is 800 Myr, which is within the error of the present estimation.

8. Synthetic CMDs

It is seen that the cluster CMD is better understood when compared with a simulated or synthetic CMD made from the evolutionary models than with isochrones. A synthetic CMD in general distributes stars along the isochrone corresponding to the age of the cluster, in accordance with the time-scale of each evolutionary state in the CMD. This feature is very useful when comparing the locations and number of stars in the red giant clump, sub-giants and stars at the tip of the turn-off. This approach can also be used to estimate the mass function of stars in the cluster.

We constructed synthetic CMDs using the theoretical stellar evolutionary models presented by Girardi et al. (2000). We used solar metallicity models to create CMDs. The algorithm used to make synthetic CMDs are presented in Subramaniam & Sagar (1995) and also used in Subramaniam & Sagar (1999). We included the effects due to binaries with mass ratio between 0.75 – 1.25 and also the photometric errors in V and (B−V). Salpeter value for the mass function, which is 2.35 (Salpeter 1955), is assumed in general. But this value could be changed to obtain the best fit when comparing the LFs. A control parameter is required to create synthetic CMD, so

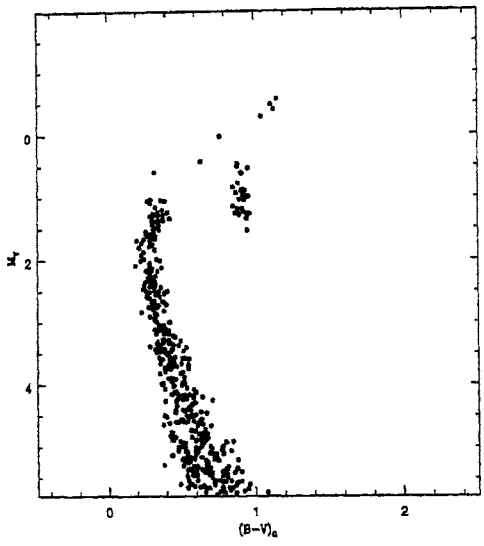

Figure 8. The synthetic CMD is shown here.

that it can be directly compared with the observed CMD. For this, one can either use the number of red giants, or the number of stars near the tip of the MS, below the turn-off. Since the red giant clump in this cluster is not very well defined and it has less number of stars, we used the stars near the top of the MS for this purpose. In the observed CMD, there are 17 stars between 15 – 15.25 in V magnitude. This is used as the control number. Initially we used a value of 30% for the fraction of binary stars in the cluster, the resulting CMDs were seen to have too many stars near the evolved part of the CMD, close to the binary isochrone path. Hence the binary fraction was reduced and a value of 10% was found to be satisfactory. Carraro& Patat (1994) have assumed a value of 15% in their synthetic CMDs.

The synthetic CMD is shown in Figure 8. The value of mass function assumed is 2.35 (Salpeter value). The synthetic CMD was initially created for an age of 890 Myr and it was found that the red giants were brighter than the ones on the observed CMD. Therefore, the age was increased to a value of 1 Gyr and the red giant magnitudes were found to match very well. Hence the synthetic CMD shown is for an age of 1 Gyr. It can be seen that the synthetic CMD mimics most of the features seen on the observed CMD. The vertical spread of the red giants is reproduced beautifully. A few stars are created on the AGB branch, but we do not see any such stars in the cluster CMD, except for the two bright and very red stars. A few stars are seen on the binary track, their number is again slightly more than what is observed, hence the value of 10% for the binary fraction could be considered as an upper limit. The stars brighter than the MS turn-off are obviously not reproduced in the synthetic CMDs, so are the stars assumed to be field stars, located on to the right and fainter end of the MS.

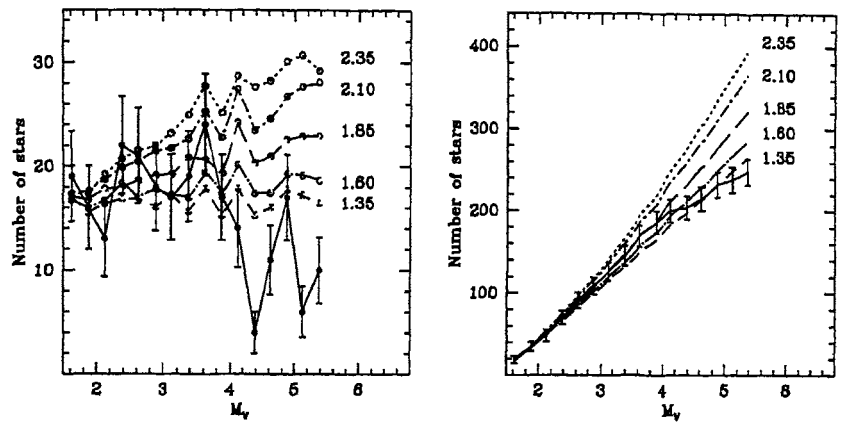

Figure 9. The synthetic LFs are shown along with the observed ones (bold lines). The left panels show LF and the right panels show ILF.

9. Luminosity Functions

As seen from the CMD of the cluster, the stellar distribution on the MS is very clumpy. In order to quantify the above, we computed the MS luminosity function (LF) by counting stars in magnitude bins on the M_V axis. The observed cluster LF profiles are shown in the left panels of Figure 9 in bold line, with statistical error at each point. The observed LF profile shows a lot of dips. At $M_V = 2.1$, 3.1 and 4.4 magnitudes, the profile dips considerably. Around $M_V = 4.4$, the number of cluster stars are found to be very minimal. The LF for a normal cluster shows an increase in the number of stars per magnitude bin from brighter magnitudes to fainter magnitudes, and this is not seen in the LF profile of NGC 1245. This is on and above the dips seen in the profile. To assess this point, we also computed the integrated luminosity function (ILF), which is cumulative in nature and hence hides smaller fluctuations. The observed ILF profile is shown in the right panel of Figure 9 as bold line marked with statistical error at each point. A closer look at the ILF profile reveals that slight kinks exist at the same magnitude levels as seen in the LF profile. The ILF profile flattens for magnitudes fainter than $M_V \geq 4.0$ mag, which corresponds to the large drop in the number of stars as seen in the LF profile.

In order to compare the LF with those predicted by stellar evolutionary model, we have computed the LFs from synthetic CMDs. The LF and ILF computed from the synthetic CMDs are plotted in Figure 9. These are shown as dotted, dashed and long dashed lines, corresponding to five different values of the mass function. It can be seen that the number of stars involved is very small, including the number of control stars used to create synthetic CMDs. This results in high statistical fluctuations in the number of stars created, which results in equally high fluctuation

in the computed LFs. Therefore, to compute reliable LFs, we have taken an average of 50 runs of the synthetic CMD and this is assumed to reduce the statistical fluctuation. As indicated by the slope of the LF, CMDs were created for Salpeter value of the mass function and for values shallower than this. Hence the CMDs were created for the mass function values of 2.35, 2.10, 1.85, 1.60 and 1.35. The value of the mass function is indicated against each LF profile computed from synthetic CMDs.

The dips seen in the observed LF profile could be due to the gaps in the MS. We see that at M_V = 2.1, no gap is noticed previously in the cluster MS. A slight dip in the simulated LFs is seen at this point, as also seen in the synthetic CMD shown in Figure 8. On the other hand, at M_V = 3.1, and $(B-V)_0$ = 0.33, there is a well-known gap called the Bohm-Vitense gap. In some clusters, this is found at a value of $(B-V)_0$ of 0.28 (Kjeldsen & Frandsen 1991), but recently some clusters were reported to have seen this gap at $(B-V)_0$ of 0.33, like Hyades (de Bruijne et al. 2000). It is interesting to note that the simulated LFs also show a dip at this magnitude. The most significant gap at M_V = 4.4 mag and $(B-V)_0$ = 0.55 is also very well seen in the observed CMD (Figure 6). In fact this gap is also seen in some old clusters like, NGC 6143, IC 4651, NGC 752 (Kjeldsen & Frandsen 1991). This luminosity corresponds to a mass of 1.15 $M_\odot$. This gap is seen in the Hyades MS also, at $M_V \sim$ 4.0 and $(B-V)$ = 0.48 and this is mentioned as the second Bohm-Vitense gap (de Bruijne et al. 2000). It is of interest to note that this gap is seen in the simulated LF. Hence the point to be noted is that there are three significant dips seen in the cluster LF, which are more or less reproduced in the simulated LFs. Therefore, there is a good chance that the gaps and hence the dips in the cluster LF are real features. It is seen that the second Bohm-Vitense gap is more prominent than the first one in this cluster.

The mass function of the cluster can be computed from the observed LF. In this cluster, due to the dips present in the LF, an estimate of the mass function was not possible. The standard plot of log(M) vs log(N) shows very large scatter and hence a straight line fit to the data points was not possible. Hence we used the ILF to estimate the mass function by comparing it with the synthetic ILF. The magnitude range considered here is between M_V = 1.5 – 5.8 magnitude. This range corresponds to a mass range of 2.2 – 0.9 $M_\odot$. The lower mass range is limited by incompleteness in the data. From the Figure it can be seen that the profile corresponding to the mass function value of 1.85 seems to fit the ILF profile better. The corresponding LF profile can also be seen to take the mean values of the observed LF. It should also be noted that, the ILF profiles for the other mass function values do not deviate very much from the observed profile at brighter magnitudes and the difference is seen mostly at the fainter ends. The observed ILF profile flattens out from the x=1.85 profile and almost touches x=1.35 profile at the fainter end at $M_V \geq$ 4.0 mag. If we ignore this large dip at the end of the ILF, and consider the range M_V = 1.5 – 4.0 mag, then the mass function value of 1.85±0.3 could be considered to fit the profile. The error in the mass function is estimated from the statistical errors in the observed profile, which happens to be within the nearby profiles corresponding to the values, 2.1 and 1.6, of the mass function slope. The effect of inclusion of the fainter stars would be to adopt a more flatter value of the mass function. Though the present estimate shows that the cluster possibly has a flatter mass function slope, an accurate estimate is not possible due to the large uncertainty seen in the fit.

Carraro & Patat (1994) found that the Salpeter value of mass function fitted the cluster ILF. The present analysis uses much more number of stars in the cluster than Carraro & Patat (1994). Since the cluster is found to have stars distributed spatially in an irregular clumps, a subsection of this cluster might not represent a true cluster sample. Hence, the present sample could be considered to be more complete. We shall discuss the possible reasons for a flatter present day mass function in the section for discussion.

10. Discussion

The estimation of cluster reddening and distance agrees quite well with those estimated by Carraro & Patat (1994). The cluster is found to be 1 Gyr old, by the synthetic CMD analysis, while Carraro & Patat (1994) found the cluster to be slightly younger than this. Wee & Lee (1996) estimated an age of 1.1±0.1 Gyr. The estimation of age by the synthetic CMD method is more reliable as it also considers the time-scale of evolution at each point on the CMD. Hence 1 Gyr could be considered as a more reliable age estimate.

The synthetic red giants are seen to be bluer than the cluster red giants. This is unlikely to arise from the error in choosing the cluster metallicity, as these red giants were found to be very close to solar metallicity. This problem may be due to the mixing length considered in the convective envelope of red giants in the model calculations, or due to error in colour-temperature relations.

The RDP is found to show that the cluster has a small deficiency of bright stars near the center of the cluster, which basically endorses the visual perception. As this cluster is 1 Gyr old, one can expect mass segregation to be present in the cluster. The core radius is estimated to be 4.75 arcmin when all stars were considered and 3.1 arcmin for stars brighter than 17.0 mag. For a distance of 3 Kpc, these correspond to 4.2 pc and 2.7 pc respectively. These values are higher than that estimated by Nilakshi et al. (2002). A smaller value for the cluster core for brighter stars, as estimated from RDP would probably point towards the presence of mass segregation.

In general, any star cluster in the Galaxy, experiences the tidal force of the Galaxy, this together with the n-body relaxation of the cluster, results in the cluster losing the low mass stars to the Galactic field. This process is accelerated due to many factors, such as dynamical friction, encounters with molecular clouds, star clusters etc. Hence over a time scale the number of low mass stars in the cluster decreases. Being an intermediate age cluster, this cluster is likely to have lost stars at the low mass end. The lost stars could also be present in the corona of the cluster. Recently Nilakshi et al. (2002) found that clusters in general have large corona and and the corona has a significant fraction of the cluster stars. The cluster area considered here is not very big and a region adjacent to the cluster region is considered as the field region. As mostly the low mass stars are spread out in the corona, the above two selection criteria could arise in under sampling and over subtracting stars at the low mass end. The flattening of the ILF at fainter magnitudes could be due to this. The present day mass function of the cluster is estimated to be 1.85, for the

brighter end and it is flatter than the Salpeter Value. One needs to see whether this value changes significantly if stars in the corona are also included.

11. Results

The summary and results of the present analysis are as follows:

1. B,V CCD photometry of 916 stars near the open cluster NGC 1245 are presented.
2. The cluster is estimated to be located at a distance of 3 Kpc, with an average reddening of E(B−V), 0.29±0.05 mag.
3. The age of the cluster is estimated to be 1±0.1 Gyr using the models from Girardi et al. (2000) and synthetic CMDs.
4. The LF of the main-sequence shows dips, which might arise due to some known gaps in the main-sequence, including the Bohm-Vitense gap.
5. The cluster is found to have a flatter present day mass function compared to the Salpeter value of 2.35.
6. The apparent paucity of brighter stars seen near the cluster center is estimated to have a statistical significance of 2 σ.

Acknowledgments

I thank the referee for comments and suggestions which improved the paper.

References

Carraro, G., Patat, F., 1994, A&A, 289, 397
Chincarini, G., 1964, Mem.S.A.It., 35, 2
de Bruijne, J.H.J., Hoogerwerf, R., de Zeeuw, P.T., 2000, ApJL, 544, L65
Girardi L., Bressan A., Bertelli G., Chiosi C., A&AS, 141, 371
Kjeldsen, H., Frandsen,S., 1991, A&AS, 87, 199
Hoag, A.A., Johnson, H.L., Iriarte, B., Mitchell, R.I., Hallam, K.L., Shapless, S., 1961, Publ. US Naval Obs., 17, 347
Lyngå, G., 1987, Catalog of Open Star Cluster Data (Strasbourg: CDS)
Nilakshi, Sagar, R., Pandey, A.K., Mohan, V., 2002, A&A, 383, 153
Salpeter, E.E., 1955, ApJ, 121, 161
Subramaniam, A., Sagar, R., 1999, AJ, 117, 937
Subramaniam, A., Sagar, R., 1995, A&A, 297, 695
Wee, S.O., Lee, M.G., 1996, JKAS, 29,181